International Journal of Physical Sciences Vol. 7(8), pp. 1187 - 1197, 16 February, 2012
Available online at http://www.academicjournals.org/IJPS
DOI: 10.5897/IJPS11.1473

Full Length Research Paper

Mapping biogenic gas concentration of Pontian Peatland, Southwest Malaysia with ground penetrating radar

Bello. Y. Idi[1,2]* and Md. N. Kamarudin[3]

[1]Department of Geomatic Engineering, FKSG, Universiti Teknologi Malaysia, Malaysia.
[2]Department of Physics, Adamawa State University, Mubi, Nigeria.
[3]Institute of Geospatial Science and Technology (INSTEG), Universiti Teknologi Malaysia, Malaysia.

Accepted 20 January, 2012

In this work, we surveyed the internal structure of peat deposit with ground penetrating radar with the aim of mapping the spatial distribution of biogenic gas produced and accumulated as a bye product of anaerobic decomposition of the deposit. The objective of the work is to identify the spatial distribution of hotspots prone to forest fire due to high concentration of the flammable gas. Four profiles of 20 m each at equidistant separation of 4 m were scanned and the radargrams obtained were processed with reflexw ground penetrating radar (GPR) processing tool. Regions of higher accumulation of biogenic gas were spatially identified based on the effect of the gas concentration on the velocity and amplitude of radar signals. Fractional volumes of the gas were numerically estimated based on complex refractive index model (CRIM). A maximum gas content of 0.1284 was obtained with a mean and variance of 0.05268 and 0.0136, respectively. Cross sectional plots of the spatial distribution of the gas were used to identify regions of anomalously higher gas content and interpreted as hotspot that are prone to forest fire. The area was generally observed to have relatively low level of biogenic gas concentration.

Key words: Ground penetrating radar, peatland, biogenic gas.

INTRODUCTION

Peat is a partially or totally decomposed accumulation of dead plants materials in marshy areas composed of marshland vegetation, trees, grasses, fungi as well as other types of organic remains under anaerobic condition. The decomposition process gradually leads to the disappearance of the physical structure and the transformation of the chemical state forming an ecosystem where the production of organic matter exceeds its decomposition. Peat soil is thus an organic soil with extremely higher proportion of organic constituents.

Peatlands are found in almost all regions of the earth but are more abundant in the higher latitude regions especially in Eurasia and North America (Objective Corporate Research, 2005). It is the most widespread of all wetlands in the world representing 50 to 70% of all global wetlands (Finlayson and Spiers, 1999). There are more than 25 million hectares of peatland in Southeast Asia comprising about 60% of the global tropical peatland resources and roughly one-tenth of the entire extent of global peat resources. The largest deposit of peatland in the Southeast Asia occurs in Indonesia which has over 70% of the total peatland resources of the region (ASEAN, 2008). Peatland is also available in many parts of Malaysia where it occurs in both highland and lowland. It is however more extensive in low lying poorly drained depression basins of the coastal areas. The total peatland area in Malaysia is approximately 2.4 million hectares, representing 8% of the country's total land area (Mamit, 2009). About 1.6 million hectares of this is found in Sarawak. Peninsula Malaysia and Sabah have peatland areas of 0.7 million and 0.1 million hectares respectively. The largest deposit of peat soil in Peninsula Malaysia is found in the state of Johor (Van-Engelen and Hutting, 2002). Peat deposit is one of the most significant

*Corresponding author. E-mail: belyus2000@gmail.com.

ecosystems in relation to vegetation, climate and green house gas regulation. Being an accumulation of dead plants, the peat absorbed carbon dioxide and stored it in the form of dead plant materials. It has been estimated that over one-third of the world's soil carbon are contained in the peat ecosystem (IMCG and IPS, 2002). About 15% of the global peatland carbon is contained in the tropical peatland alone (Mamit, 2009). The drainage of peatland therefore leads to the oxidation of carbon dioxide which is released into the atmosphere. One of the major environmental challenges of Asian countries including Malaysia is the issue of forest fire facilitated by degradation of pealand. Forest fire occurs at many peatland forests at pineapple plantations in Malaysia since 1970s (Nuruddin, 1998). The most prominent incidence is the 1997/1998 El-nino disaster which affected many countries of the Southeast Asia. The disaster destroyed about 10% of the total peatland areas of Indonesia (UNEP and GEF 2005). Four incidences of forest fire were recorded in Peninsula Malaysia during the 1997/1998 El-nino disaster with a total burnt area of 425.27 ha (Nuruddin, 1998). The Centre for International Forestry Research (CIFOR) in Jakarta, Indonesia, where the fire originated from, reported that the cause of the fire was from unconsolidated peat burning (Rowell and Moore, 2000).

It is in the realization of the environment impact of peatland degradation that at the 9th Asian Ministerial Meeting on Haze held on 11th June, 2002, it is agreed that the Asian Peatland Management Initiative (APMI) be established with the goal of promoting sustainable management of peatland in the Asian region (ASEAN, 2008). The objective of the initiative is to reduce the incidence of forest fire and its associated haze through the promotion of activities for the enhancement of sustainable peatland management and fire prevention. Subsurface mapping of the spatial distribution of biogenic gas is a step toward realizing the objectives of APMI initiative.

In this work, we conducted subsurface survey with ground penetrating radar (GPR) with the aim of mapping the internal structure of a peat soil. The objective of the work is to map the spatial distribution of biogenic gas in the interior of the deposit for the purpose of identifying hotspots regions that are prone to forest fire due to high concentration of the inflammable gas. The work therefore provides useful information necessary for effective management and sustainable development of the peat resource.

METHODOLOGY

Theoretical framework

GPR is a near surface geophysical tool that record the back scattered signal of the subsurface reflected due to contrast in the electrical properties of the earth composition. It records continuous graphic profiles of the subsurface interfaces with high degree of accuracy. The technique is widely applicable for effective detection of buried objects and characterization of subsurface structures. These include among others: detection and inspection of structural elements and weaknesses of historical building (Barone et al., 2010), mapping and modeling terrace deposits and other geologic features (Tye et al., 2011), outlining the foundation of buildings and other engineering structures (Abbas et al., 2009), monitoring and controlling coastal environment by imaging shallow Holocene sediment for lake level change detection (Kanbur et al., 2010), location of water table, and characterization of subsurface contamination (Hamzah et al., 2009) etc.

The suitability of GPR as a geophysical survey tool is strongly influenced by the electrical and hydrogeological properties of the subsurface. Peat is characterized by low magnitude of electrical conductivity due to the presence of highly concentrated inactive and strongly bound organic compounds. The low level of electrical conductivity enables larger depth of penetration. Studies on peatland imaging with GPR have recorded remarkable achievements. For instance Pelletier et al. (1991) delineated peat boundaries in the Hudson Bay lowlands of Canada using both ground and air-borne GPR data. Better result was obtained from the ground-based data as the interface between the peat and the older deeper marine clays were accurately determined due to the conductivity differential between them. They were also able to delineate stratifications within the peat deposit. The work also reveals the successive variation in the rate of decomposition of organic material content that makes up the peat and hence indicates the possibility of variation in the organic nutrient content. Dallaire et al. (2009) used GPR to obtain a continuous representation of the dominant stratigraphic layers of peat and its associated carbon attributes for the estimation of carbon pool in Lac Le Caron peatland, Canada. Stratigaphic layers within the peat were identified from the radargram. Peat core analysis was used to interpolate the stratigraphic changes with the carbon pool and relate it with the fen/ bog transition (transition of the wet marshy area).

A parameter of primary importance in GPR exploration is the radar propagation velocity across the medium of investigation. Radar propagation velocity v is determined by the relative dielectric permittivity of the material medium. Relative dielectric permittivity is the measure of the polarization or reorientation of the molecules of the medium due to the influence of the applied electric field. Within GRP frequency range, the real component of dielectric constant (dielectric permittivity) of a material ε_r is given by (Grote et al., 2002).

$$\varepsilon_r = \left(\frac{c}{v}\right)^2 \quad (1)$$

where c and v are respectively the velocities of EM waves in free space and the material medium.

Hydrogeological parameters such as water content porosity etc are estimated based on empirical relationship between them and the dielectric permittivity of the soil matrix. Water content of a soil can be estimated using the famous Topp's equation relating the dielectric permittivity ε_r of soil formation with its water content θ given as (Pumpanen and Llvesniemi, 2005)

$$\theta = a + b\varepsilon_r + c\varepsilon_r^2 + d\varepsilon_r^3 \quad (2)$$

where the parameters *a, b, c*, and *d* are constants for many soil materials. It is however observed that organic soils such as peat tend to deviate from the Topp's empirical equation (Jol, 2009). The deviation of clay and organic soil including peat from Topp's equation was attributed to some factors uniquely affecting the relationship between water content and dielectric permittivity of unconsolidated deposit. These include among others: significantly high imaginary part of the relative permittivity of the soil and high content of bound water with lower relative permittivity than free water (Cosenza and Tabbagh, 2004). Topp's relationship is therefore not applicable to organic soils and layers such as peats and forest floors.

To estimate the water content of organic soil, many empirical equations were developed for the dielectric constant – water content relationship mainly based on time domain reflectometry (TDR) instrumentation. Pumpanen and Ilvesniemi (2005) calibrated two most prominent of such equations relative to Topp's equation with experimental data using least square fitting method. The model equations are:

Leidieu model equation: $$\theta = a\sqrt{\varepsilon_r} - b \qquad (3)$$

Logarithmic model equation: $$\theta = a\ln\varepsilon_r - b \qquad (4)$$

where *a* and *b* are fitting parameters depending on the soil type. With a fitting coefficient R^2 of 0.968, the logarithmic model was found to have the best fit that described the relationship between water content and dielectric constant compared to other models. For poorly compacted organic soil like peat, the mean values of the parameters *a* and *b* were numerically estimated as 0.188 and 0.120, respectively.

The biogenic gas compositions of the peat are mainly CH_4 and CO_2; the two most important global warming potential gases that are in some cases emitted to the environment. The frequent cases of forest fire are partly attributed to the accumulation of the flammable components of these gases. Thus identification of hotspots related to high concentration of these biogenic gases is an effective step toward management, control and prevention of forest fire. Surface GPR test together with moisture probe laboratory analysis were used by Comas et al. (2005) to detect areas of biogenic gas accumulation in a peatland. The aim was to observe the effect of the gas accumulation on GPR signals. Observation showed that areas of higher accumulation of CH_4 and CO_2 coincide with high velocity zones and are also characterized by shadow zones of the radargram. Thus higher signal velocity and amplitude blanking zones are indicative of higher biogenic gas accumulation.

The free-phase gases, which are products of microbial activities within the subsurface of the peat displaces water from the saturated pore space. The fractional gas content at a given spatial location is numerically given as the difference between the porosity and water content (Comas and Slater, 2009). An empirical relationship between these quantities and the petrophysical properties of the peat is given by complex refractive index model (CRIM) which applied mixing model for estimating the dielectric properties of the soil matrix, its constituents and volumetric properties of the soil. The model formula as given by Comas et al. (2005) and Parsekian and Slater (2009) expresses the effective dielectric property ε_r of the medium as

$$\varepsilon_r = [\theta\varepsilon_w^\alpha + (1-\varphi)\varepsilon_s^\alpha + (\varphi-\theta)\varepsilon_a^\alpha]^{1/\alpha} \qquad (5)$$

where ε_s, ε_a and ε_w are the respective dielectric properties of the soil, air (= 1) and water (= 81). φ is the porosity of the medium and θ is the water content. The factor α is the fitting parameter depending on the orientation of the electric field relative to the medium geometry of the particle arrangement and is numerically found to be 0.32 for peat soil based on previous study. The dielectric constant of organic peat soil ε_s was also experimentally found to be 2.5 (Parsekian and Slater, 2009). The quantity $(\varphi - \theta)$ is described by Comas and Slater (2009) as the measure of the volumetric quantity of the biogenic gas content according to the model.

Study area

The study area is a 240 m^2 plot of peatland located along Pontian-Pekan Nanas highway, near Kampung Batu Dua Puluh Sembian at Pontian district, in the state of Johor, Malaysia (longitude 103°27'49.94"E to 103°27'38.88"E and latitude 1°35'15.16"N - 1°35'08.14"N). The area (Figure 1) is topographically flat lowland within the low vegetation cover and is geologically within the Johor Bahru - Kulai map covered by sheet 130 map bulletin of the Geological Survey of Malaysia. According to the map, about 83% of the area's topography is lowland characterized by undulating topography. The area is a portion of the coastal plain of southwestern Johor described by ASANUS (1991) as largely underlain with marine clay, silt and the paludal peat deposit of Holocene age. Being the southernmost district in the state which is at the southern tip of peninsula Malaysia, the area is bounded to the southwest by the strait of Melaka which separates it from one of the main islands of Indonesia. The area is one of the wettest parts of the state. Heaviest rainfall in southern Johor is recorded in northeastern parts of the area and Kota Tinggi (ASANUS, 1991). The land utilization in the area is mainly agriculture.

Data acquisition and interpretation

A common offset single fold reflection profiling was used to obtain a GPR cross section along four equidistant profiles (P1, P2, P3 and P4) running in the east-west direction at the surface of the area (Figure 1). Each profile is of length 20 m and the interval between profiles is 4 m. The data were acquired using IDS DAD fast wave radar acquisition unit at a fixed centre frequency of 200 MHz. The area was scanned at a trace increment of 0.025 within 100 ns time window. A perpendicular polarized broadside antenna orientation was used throughout the operation. Figure 2 shows the raw radar image obtained along the four profiles. The first strong arrival that occurs at a time scale range of 5 to 15 ns in all the profiles is direct waves from the source to the receiver which can be removed using static correction. Strong reflections are discernible between 15 ns to about 40 ns time scale.

The acquired data images were processed with Reflexw GPR/seismic processing software. Temporal filtering (dewow) was applied to remove very low frequency components from the data. Low and high frequency noises were removed using bandpass butterworth filter. Background removal was applied in order to eliminate temporarily consistent noise. Time gain was also applied to compensate for the signal attenuation with depth. This equalizes the amplitudes decay with depth. In applying the time gain, the signal amplitude was observed on a section bases. Automatic gain control (AGC) was used for this work. No migration was applied to the data in order to preserve the hyperbolic diffraction pattern needed for velocity adaptation. The processed radar images are shown in Figure 3a to d. Velocity adaptation of the diffraction hyperbolas were used to estimate the radar velocity and a mean value of 0.069 m/ns was obtained. The value was used to convert the vertical time axis to depth axis leading to a maximum depth of 3.45 m.

Regions of biogenic gas accumulation were identified based on the effect of the gas accumulation on radar signals. The signal blanking associated with gas accumulation described in detail by Comas et al. (2005) was independently confirmed by Tsofias et al. (2010) in a 90-day laboratory scale experiment using biostimulation reactor. The results show rapid increase in signal attenuation in

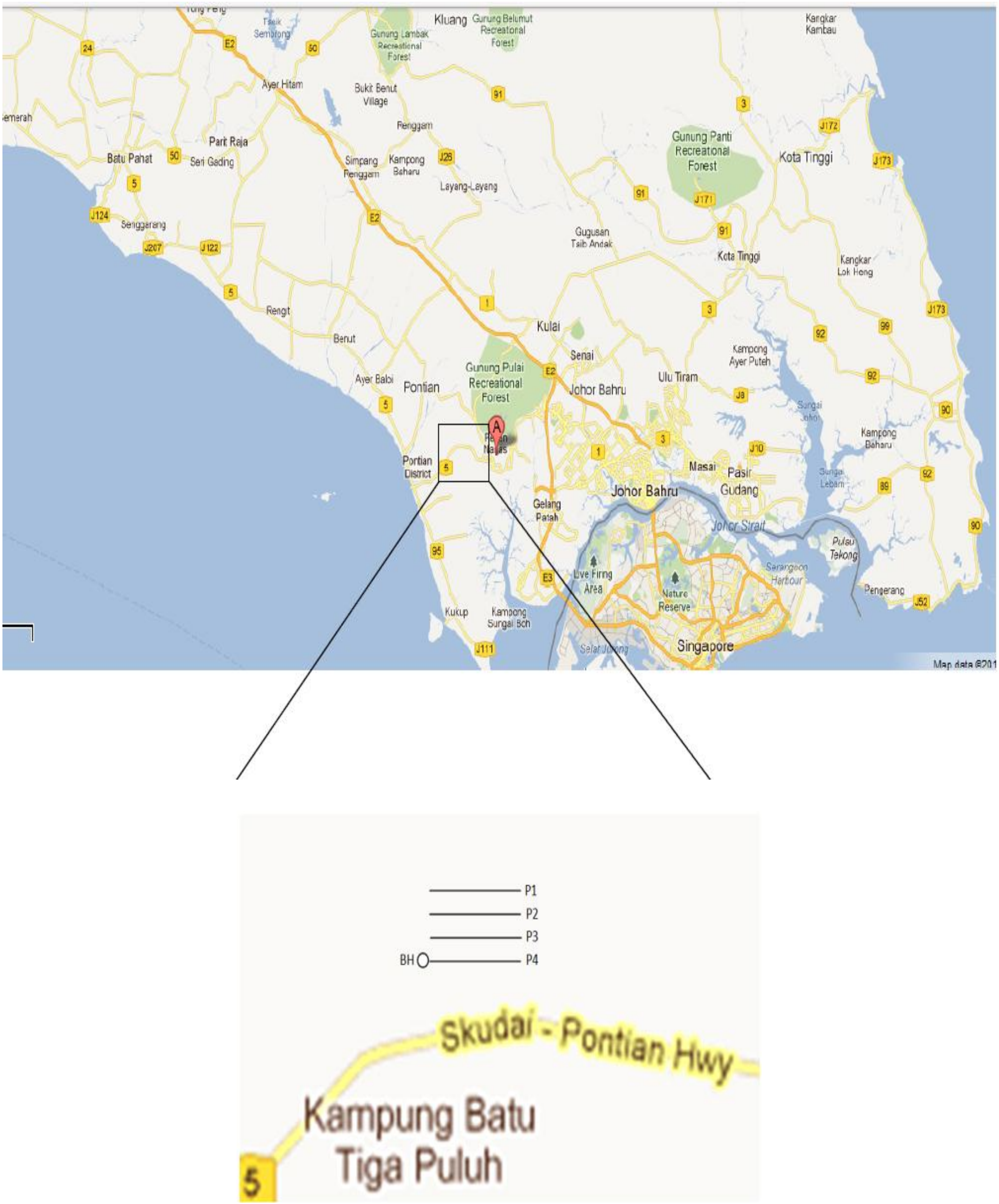

Figure 1. Map of the study area (Google map).

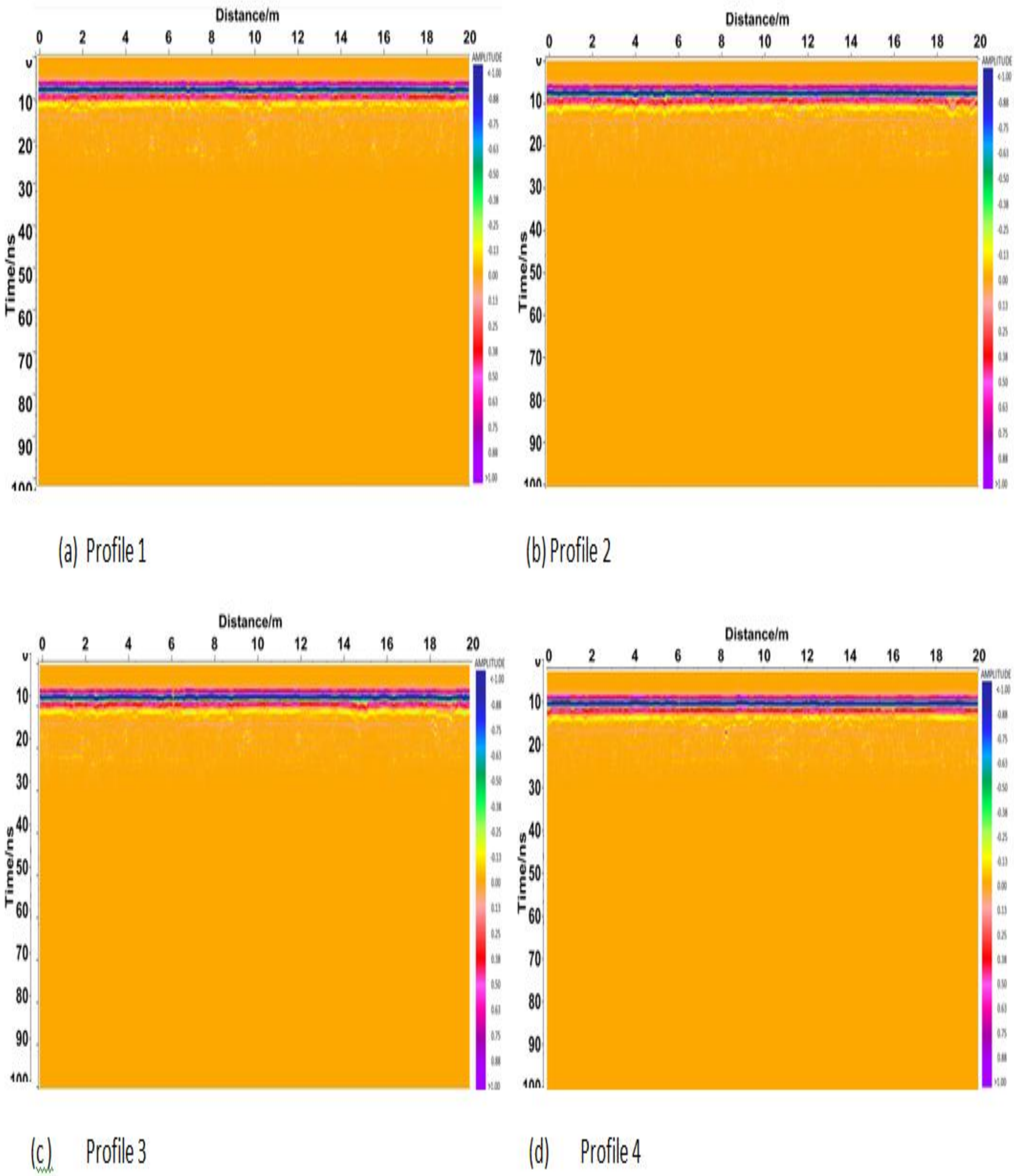

Figure 2. Raw radar images acquired at the four profiles (a) Profile 1; (b) profile 2; (c) profile 3; (d) profile 4.

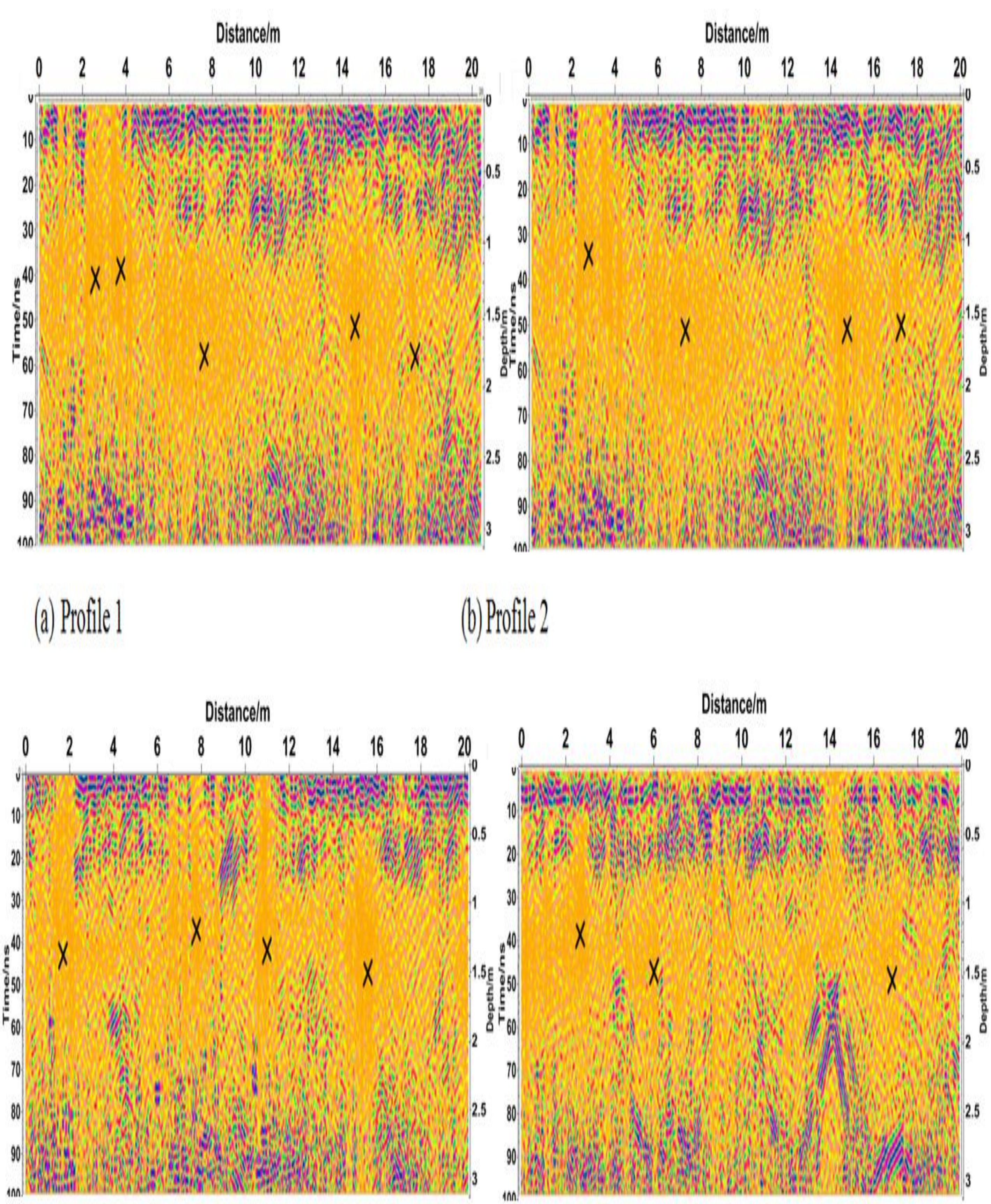

Figure 3. Processed radar image with signal shadow zones marked as expectedly regions of high biogenic gas content.

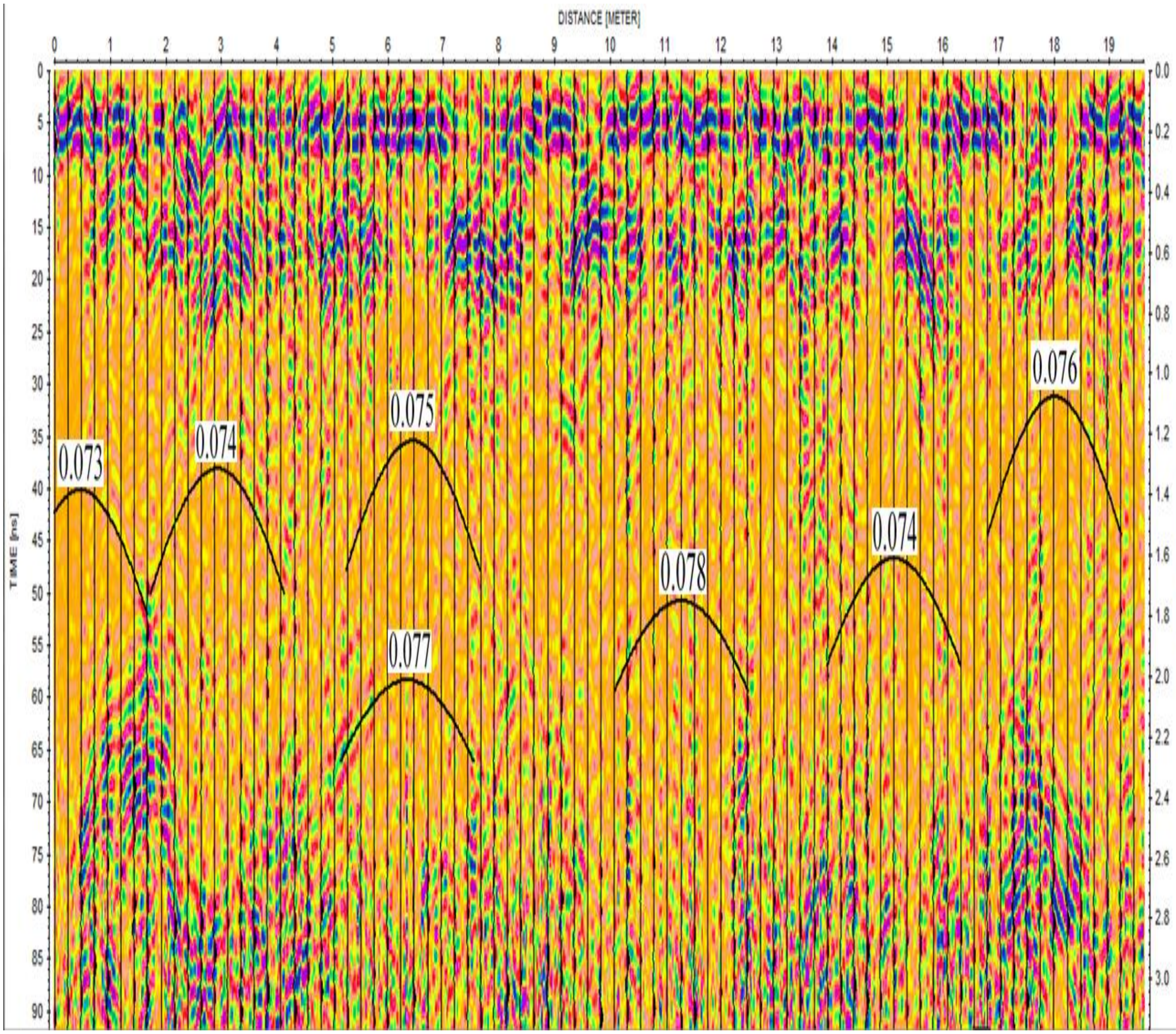

Figure 4. Hyperbolic fitting of reflection hyperbolas within the shadow zones of Profile 1.

the vicinity of biogenic gas which was attributed to increase in electrical conductivity of the pore fluid. They also observed that radar velocity increases rapidly as a result of the formation of biogenic gas in the pore space.

The shadow zones suspected to be associated with biogenic gas accumulation are clearly visible in the processed radargram as regions of weak signal reflections marked X in Figure 3. Accumulation of biogenic gas may however not be the only factor responsible for the signal attenuation. Hence velocity information was also used as further criterion. Regions of higher signal velocity within the shadow zones were interpreted as the regions with considerable accumulation of the gas.

Fractional volumes of the gas were numerically estimated based on CRIM model (Equation 5) as the difference between porosity and water content at each identified location. The procedure involves estimation of radar signal velocity using velocity adaptation for all reflection hyperbolas discernible within the shadow zones in the processed radargram and subsequent conversion to dielectric constant using Equation (1). Figure 4 is a window snapshot of the velocity adaptation obtained by fitting reflection hyperbolas within the shadow zones of Profile 1. The signal blanking regions are made more identifiable with wiggle mode plot which gives polygonal line traces of size corresponds to the mean amplitudes. The dielectric constant obtained was used to compute the water content based on logarithmic model (Equation 3). The water content and the matrix dielectric constant ε_r obtained together with the numerical values of the constant parameters were used in Equation(5) to compute the porosity.

RESULTS

Table 1 gives the numerical values of radar velocities obtained from the hyperbolic fittings and their corresponding dielectric constants, water contents and porosities for the four profiles. The computed fractional gas volume is also shown in the Table. Figure 5 is across

Table 1. Computed results.

X/m	Y/m	Velocity (/ns)y	Dielectric	Water content	Porosity	Gas content
Profile 1						
0.5	-1.38	0.073	16.8887	0.4114	0.4041	0.0073
3.0	-1.3	0.0740	16.4354	0.4063	0.4207	0.0144
6.2	-1.21	0.075	16.0000	0.4012	0.4365	0.0353
6.3	-2.0	0.077	15.1796	0.3914	0.4660	0.0747
11.3	-1.75	0.078	14.7929	0.3865	0.4798	0.0933
15.1	-1.8	0.074	16.4354	0.4063	0.4207	0.0144
18.0	-1.8	0.076	15.5817	0.3963	0.4516	0.0554
Profile 2						
1.0	-0.60	0.076	15.5817	0.3963	0.451629	0.0554
3.1	-1.14	0.077	15.1796	0.3914	0.466049	0.0747
3.7	-1.58	0.079	14.4208	0.3817	0.492916	0.1112
6.6	-1.45	0.074	16.4354	0.4063	0.420674	0.0144
6.9	-2.17	0.070	18.3674	0.4273	0.349406	-0.0778
14.2	-1.24	0.075	16.0000	0.4012	0.436514	0.0353
14.2	-1.85	0.077	15.1796	0.3914	0.466049	0.0747
16.8	-1.58	0.076	15.5817	0.3963	0.451629	0.0554
Profile 3						
1.7	-0.55	0.075	16.0000	0.4012	0.4365	0.0353
1.7	-1.35	0.073	16.8887	0.4114	0.4041	-0.0073
6.8	-1.45	0.076	15.5817	0.3963	0.4516	0.0554
6.8	-1.50	0.078	14.7929	0.3865	0.4798	0.0933
10.8	-1.40	0.078	14.7929	0.3865	0.4798	0.0933
11.0	-0.75	0.075	16.0000	0.4012	0.4365	0.0353
15.2	-1.18	0.074	16.4354	0.4063	0.4207	0.0144
19.7	-1.52	0.074	16.4354	0.4063	0.4207	0.0144
Profile 4						
2.1	-1.22	0.076	15.5817	0.3963	0.4516	0.0554
2.7	-0.84	0.078	14.7929	0.3865	0.4798	0.0933
4.9	-1.28	0.074	16.4354	0.4063	0.4207	0.0144
9.2	-1.35	0.079	14.4208	0.3817	0.4929	0.1112
13	-1.50	0.075	16.0000	0.4012	0.4365	0.0353
14.7	0.95	0.077	15.1796	0.3914	0.4660	0.0747
17.2	-1.68	0.080	14.0625	0.3770	0.5054	0.1284

sectional plots of the spatial distribution of the biogenic gas content obtained for the four profiles.

The cross sectional plots indicate regions of higher concentration of the gas as closures and lineaments of contour highs within the subsurface. Figure 8 is an image map of lateral variation in the spatial distribution of the gas content covering the area. The plotted values are the mean values of the gas content that coincide within a vertical positions. Regions of higher concentration of the gas were spatially imaged as shown in the map.

DISCUSSION

With a maximum recorded content of about 12.8%, the gas content can generally be described as low within the study area. The subsurface cross sectional plots give the distribution of the free –phase gas concentration across the mapped profiles. Regions of higher gas content are regarded as hotspots with the higher probability of accordance of forest fire. A hotspot region is clearly visible in Profile 1 at a horizontal position and depth of about 11 and 1.8 m respectively with a recorded value of 0.0933. Thus a maximum gas content of about 9.33% is recorded across the profile. Higher volumetric gas content was recorded across Profile 2 with a maximum value of 11.12% at the closure of contour highs within a horizontal position and depth of about 3.8 and 1.7 m, respectively. Maximum gas content of about 9.33% was

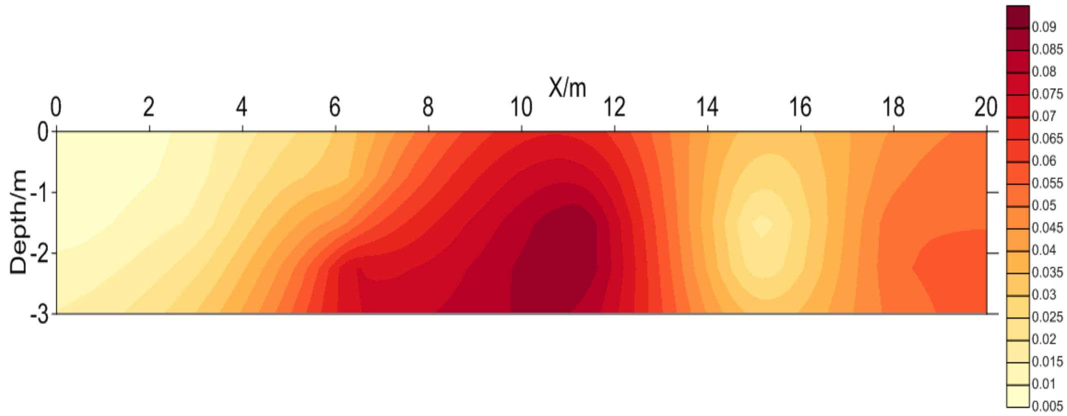

(a) Profile 1

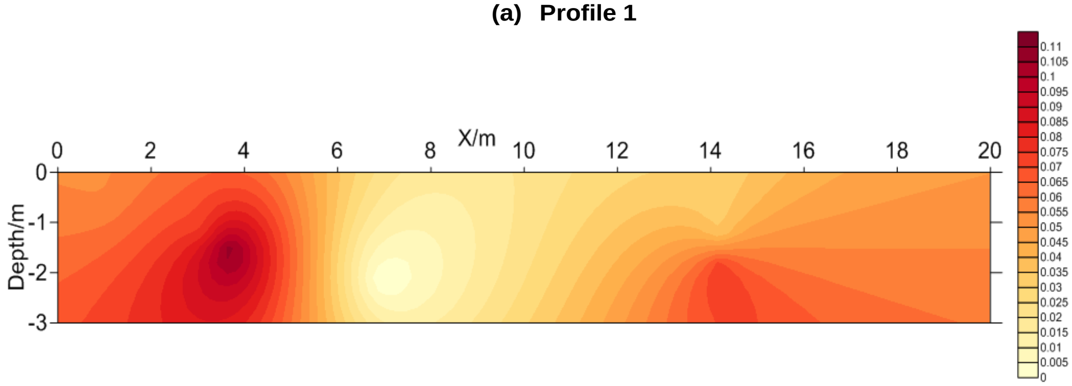

(b) Profile 2

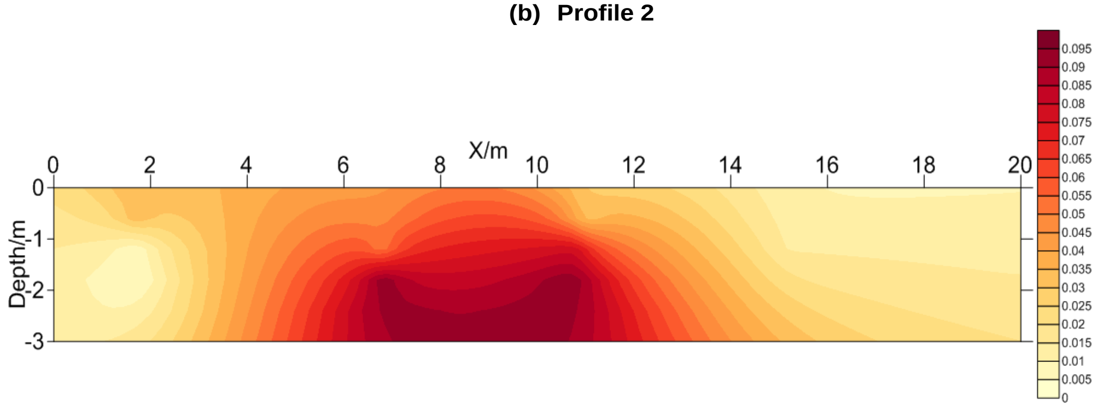

(c) Profile 3

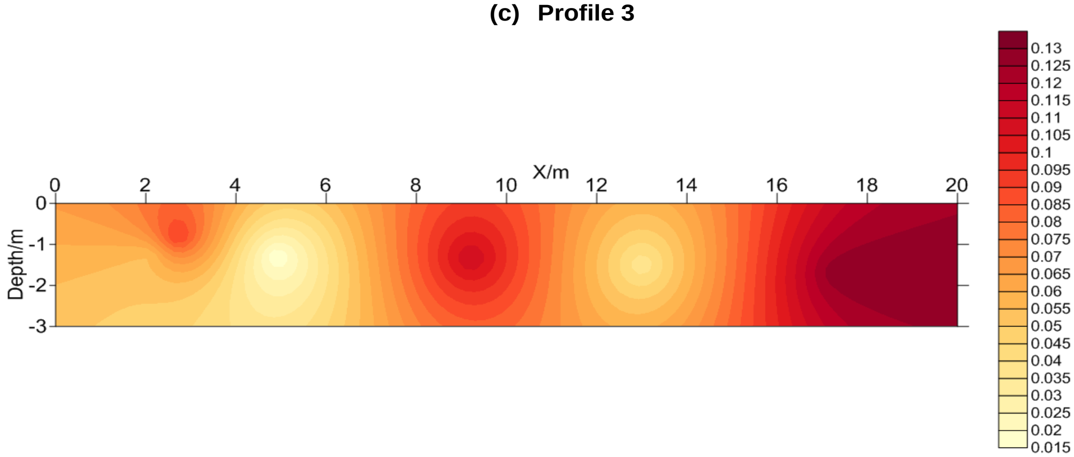

(d) Profile 4

Figure 5. Cross sectional plots of biogenic gas distributions.

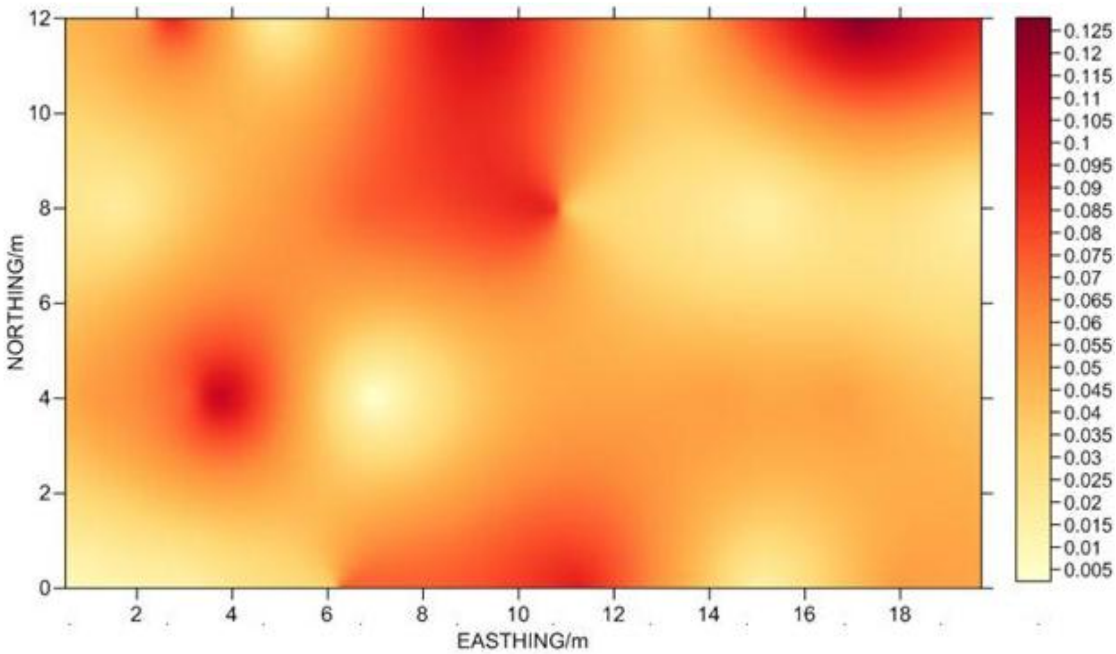

Figure 6. Image map of spatial distribution of the hotspots.

recorded in two regions of Profile 3 at nearly the same depths of about 1.4 and 1.5 m. They both appear as regions of contour highs at about 6.8 and 10.8 m horizontal positions respectively. The highest volumetric gas content of about 12.84% was recorded in the cross section of Profile 4 at a horizontal position and depth of about 17.2 and 1.68 m, respectively. This region appears as lineament of contour highs that continue to the extreme end of the profile.

As stated earlier, the presence of biogenic gas may not be the only factor responsible for signal attenuation. Factors such as high concentration of organic nutrient, salinity and other dissolved ions in the groundwater enhance electrical conductivity and cause signal attenuation. Increase water content on the other hand enhances permittivity of the soil matrix due to high content of polarizable water molecules. Thus both the permittivity and conductivity of the peat soil increase when saturated with mineralized water. Regions of high concentration of mineralized water under saturation condition could equally appear as shadow zones in the radar image. Low radar velocity is however expected within these regions due to increased permittivity. Two of such regions were detected at 6.9 m distance and 2.17 m depth of Profile 2; and 1.7 m distance and 01.35 m depth of Profile 3. Radar velocities of 0.070 and 0.073 m/ns were respectively recorded at the two points. It is expected that at saturation where the pore spaces are completely filled with water, the biogenic gas content should be zero. But at these points, and other velocity values below 0.074 m/ns, recorded volumetric water content was higher than porosity. Such regions are considered water saturated with minimum or zero quantity of biogenic gas. This is based on the fact that a very porous soil can have water content greater than 100% when saturated (Powers et al., 2007).

Hotspot delineation is more noticeable in the 2-D image map (Figure 6) which spatially shows the lateral distribution of the biogenic gas across the entire study area. The map clearly shows about six regions of anomalously high gas content at different spatial locations. With a mean and variance of volumetric gas content of about 5.268% and 0.0136 respectively, the biogenic gas content of the study area can generally be described as low. GPR surveying technique over peatland is therefore another hotspot monitoring system which provides hotspot data that serves as an indication of forest fire probability.

Conclusion

In this work, we assessed the internal structure of the peat soil for the purpose of mapping the biogenic gas concentration, a major constituent of the peat soil which is accumulated and trapped within the porous media of the deposit. GRP image was acquired across four profiles over a peatland of area 240 m^2. The radar image obtained was processed and enhanced with the basic processing tools of the reflexw software. Biogenic gas accumulations were quantified using CRIM model which relate the petrophysical properties of the peat matrix with hydrogeological parameters. Cross sectional plots of the spatial distribution of biogenic gas concentration for all the profiles were used to identify regions of anomalously higher gas concentration and marked as hotspot regions that are prone to forest fire. Although the work is limited by the relatively small depth of coverage, the results obtained indicate the effectiveness of GPR as a tool for spatial delineation of biogenic gas concentration in peatland.

ACKNOWLEDGEMENTS

The authors acknowledged with thanks the contribution of Jurukur Abadi of No. 06-01, Jalan Padi Emas 4/5, Pusat Bandar Tampoi, 81200 and Johor Bahru for the test data acquisition.

REFERENCES

Abbas AM, Kamei H, Helal A, Atya MA, Shaaban FA (2009). Contribution of geophysics to outlining the foundation structure of the Islamic Museum, Cairo, Egypt Archaeol. Prospect. 12(3): 167-176.

ASANUS (1991). The Coastal Environmental Profile of South Johore, Malaysia.Association of SoutheastAsian Nations/United States, Coastal Resources Management Project,Technical Series 6.

ASEAN (2008). Sustainable Management of Peatlands: Wise Use, Prevention of Fire and Rehabilitation.A Contribution to the Implimentation of the ASEAN Agreement on Transboundary Haze Pollution and the ASEAN Regional Haze Action Plan. ASEAN Peatland Management Initiative; Jakarta, Indonesia, p. 3.

Barone PM, Matteo AD, Graziano F, Mattei E, Pewttinelli E (2010). GPR application to the structural control of historical buildings: two case studies in Rome, Italy. Near Surf. Geophys., 8(5): 407-413.

Comas X, Slater L (2009). Non-Invasive field-scale characterization of gaseous-phase methane dynamics in peatlands using the Ground Penetrating Radar (GPR) Cycling in Northern Peatlands, Geophysical Monograph 184, American Geophysical Union (AGU). pp. 159-172.

Comas X, Slater L, Reeve A (2005). Spatial variability in biogenic gas accumulations in peat soils is revealed by ground penetrating radar (GPR). Geophys. Res. Lett., p. 32. L08401, doi: 10.1029/ 2004GL022297.

Cosenza P, Tabbagh A (2004). Electromagnetic determination of clay water content: role of the microporosity. Appl. Clay Sci., 26: 21-36.

Dallaire P, Garneau M, Giroux B (2009). High-resolution carbon pool estimation at peatland scale using ground-penetrating radar and paleoecological data. In: the 2nd International Symposium: Peatlands in the Global Carbon Cycle Praha, Czech Republic, pp. 25-30.

Finlayson CM, Spiers AG (1999). Global Review of Wetland Resources and Priorities for Wetland Inventory. Supervising Scientist Wetlands International Publication 53, Supervising Scientist, Canberra, pp. 520.

Grote K, Hubbard S, Rubin Y (2002). GPR monitoring of volumetric water content in soils applied to highway construction and maintenance. Leading Edge. pp. 482-504.

Hamzah U, Ismail MA, Samsudin AR (2009). Geoelectrical resistivity and ground penetrating radar techniques in the study of hydrocarbon-contaminated. Soil Sains Malaysiana, 38(3): 305–311.

IMCG, IPS (2002). Statement on the Wise Use of Peatlands. Prepared by the International Peat Society and International Mire ConservationGroup.from http://www.imcg.net/docum/wise0204.pdf

Jol HM (2009). Ground Penetrating Radar Theory and Applications. Elsevier Science, Amsterdam, the Neitherlands, p. 208.

Kanbur Z, Gormus M, Kanbur S, Durhan Z (2010). Significance of shallow seismic reflection (SSR) and ground penetrating radar (GPR) profiling on the Modern Coast line History of the Bedre area, Egirdir Lake, Isparta, Turkey. J. Asian Earth Sci., 38: 262–273.

Mamit JD (2009). Peatland Utilization in Malaysia: the Present Status. IPS meeting.

Nuruddin AA (1998). Forest Fire in Malaysia: an Overview. IFFN 18: 51-52.

Objective Corporate Research (2005). The Peat Industry Alternative Energy Out of the Bog. Introducing Peat Resources (PET.V) Objective Capital Limited, UK. Corporate: www.ObjectiveCapital.comrofil.

Parsekian A, Slater L (2009). A comparison of 1D vertical models of biogenic gas content within a northern peatland from common mid-point and cross-borehole GPR. IEEE. 978-1-4244-4605.

Pelletier RE, Davis JL, Rossiter JR (1991). Peat analysis in the Hudson Bay Lowlands using gound penetrating radar. IEEE, CH2971-0/91/0000-2141.

Powers JP, Corwin AB, Schmall PC, Kaeck WE (2007). Construction Dewatering and Groundwater Control: NewMethods and Applications, 3rd Edition. John wiley 7 sons inc, Hoboken, New Jersey.

Pumpanen J, Llvesniemi H (2005). Caliberation of time domain reflectometry for forest humus layers. Boreal Environ. Res., 10: 589-595.

Rowell A, Moore PF (2000). Global Review of Forest Fires. WWF and IUCN report. Gland, Swizerland, p. 35.

Tsofias G, Schillig P, McGlashan M, Roberts J, Devlin J (2010). Field and Laboratory GPR Monitoring of Biological Activity in Saturated Porous Media. Geophys. Res. Abstr., 12: EGU2010-6415-1.

Tye AM, Kessler H, Ambrose K, Williams JDO, Tragheim D, Scheib A, Raines M, Kuras O (2011). Using integrated near-surface geophysical surveys to aid mapping and interpretation of geology in an alluvial landscape within a 3D soil-geology framework. Near Surf. Geophys., 9(1): 15-31.

UNEP, GEF(2005). Wetland International, Global Environment Centre Peat Matters Selango, Malaysia. p. 2.

Van-Engelen V, Hutting J (2002). Peatlands of the World. An interpretation of the World Soil Map. ISRIC, Wageningen and GPI Project 31 GP1.